ANTICANCER RESEARCH *38*: 4459-4467 (2018)
doi:10.21873/anticanres.12748

Quantitative Structure–Cytotoxicity Relationship of 3-(*N*-Cyclicamino)chromone Derivatives

HAIXIA SHI[1,2*], JUNKO NAGAI[3*], TSUKASA SAKATSUME[4], KENJIRO BANDOW[5], NORIYUKI OKUDAIRA[6], YOSHIHIRO UESAWA[3], HIROSHI SAKAGAMI[2], MINEKO TOMOMURA[5], AKITO TOMOMURA[5], KOICHI TAKAO[4] and YOSHIAKI SUGITA[4]

[1]*Department of Traditional Chinese Medicine, Shanghai Ninth People's Hospital, Shanghai Jiatong University School of Medicine, Shanghai, P.R. China;*
[2]*Meikai University Research Institute of Odontology (M-RIO), Saitama, Japan;*
[3]*Department of Medical Molecular Informatics, Meiji Pharmaceutical University, Tokyo, Japan;*
[4]*Department of Pharmaceutical Sciences, Faculty of Pharmacy and Pharmaceutical Sciences, Josai University, Saitama, Japan;*
Divisions of [5]*Biochemistry and* [6]*Pharmacology, Meikai University School of Dentistry, Saitama, Japan*

Abstract. *Background/Aim: 4H-1-Benzopyran-4-ones (chromones) provide a backbone structure for the chemical synthesis of potent anticancer drugs. In contrast to 2-(N-cyclicamino)chromones, the biological activity of 3-(N-cyclicamino)chromones has not been reported. In this study, cytotoxicity of 15 3-(N-cyclicamino)chromone derivatives was investigated and subjected to quantitative structure–activity relationship (QSAR) analysis. Materials and Methods: Cytotoxicity against four human oral squamous cell carcinoma cell lines and three oral normal mesenchymal cells was determined by the 3-(4,5-dimethylthiazol-2-yl)-2,5-diphenyltetrazolium bromide (MTT) method. Tumor-specificity (TS) was evaluated as the ratio of mean 50% cytotoxic concentration (CC_{50}) against normal oral cells to that against human oral squamous cell carcinoma cell lines. Potency-selectivity expression (PSE) value was calculated by dividing the TS value by the CC_{50} against tumor cells. Apoptosis induction was evaluated by morphological observation, western blot analysis and cell-cycle analysis. For QSAR analysis, a total of 3,096 physicochemical, structural and quantum chemical features were calculated from the most stabilized structure optimized using CORINA. Results: 3-(4-phenyl-1-piperazinyl)-4H-1-benzopyran-4-one (**3a**) had the highest tumor specificity, comparable with that of melphalan, without induction of apoptosis. Compound **3a** caused cytostatic growth inhibition and had much lower cytotoxicity against human oral keratinocytes compared to doxorubicin. TS of the 15 3-(N-cyclicamino)chromones was correlated with 3D structure and lipophilicity. Conclusion: Chemical modification of **3a** may be a potential choice for designing a new type of anticancer drug.*

*These Authors contributed equally to this work.

Correspondence to: Haixia Shi, Department of Traditional Chinese Medicine, Shanghai Ninth People's Hospital, Shanghai Jiatong University School of Medicine, 280, Mohe Road, Shanghai, 201900, P.R. China. E-mail: haixia.0101@163.com; Hiroshi Sakagami, Meikai University Research Institute of Odontology (M-RIO), 1-1 Keyakidai, Sakado, Saitama 350-0283, Japan. Tel: +81 492792758 (office), +81 492792787 (M-RIO)(dial-in), Fax: +81 492855171, e-mail: sakagami@dent.meikai.ac.jp

Key Words: 3-(*N*-Cyclicamino)chromones, QSAR analysis, cytotoxicity, tumor selectivity, apoptosis induction, molecular shape.

4*H*-1-Benzopyran-4-one (chromone), found ubiquitously in the plant kingdom (1), provides a backbone structure for synthesis of various derivatives. We reported that 3-styrylchromones (2), 3-styryl-2*H*-chromenes (3) and 22-azolylchromones (4), had much higher cytotoxicity against human oral squamous cell carcinoma (OSCC) cell lines than against human normal oral mesenchymal cells (gingival fibroblast, periodontal ligament fibroblast, pulp cell), yielding excellent tumor specificity, comparable with that of several anticancer drugs (5).

2-Aminochromone derivatives are reported to have various biological activities including anti-inflammatory activity (6, 7), antimicrobial activity (8), phosphodiesterase inhibition (8, 9), modulation of DNA repair (10), inhibition of DNA-dependent protein kinase and radiosensitization of a human tumor cell line (11), and as potential positron-emission tomographic agents for imaging of DNA-dependent protein kinase in cancer (12). We recently found that among 15 such 2-(*N*-cyclicamino)chromone derivatives, 7-methoxy-2-(4-morpholinyl)-4*H*-1-benzopyran-4-one had the highest

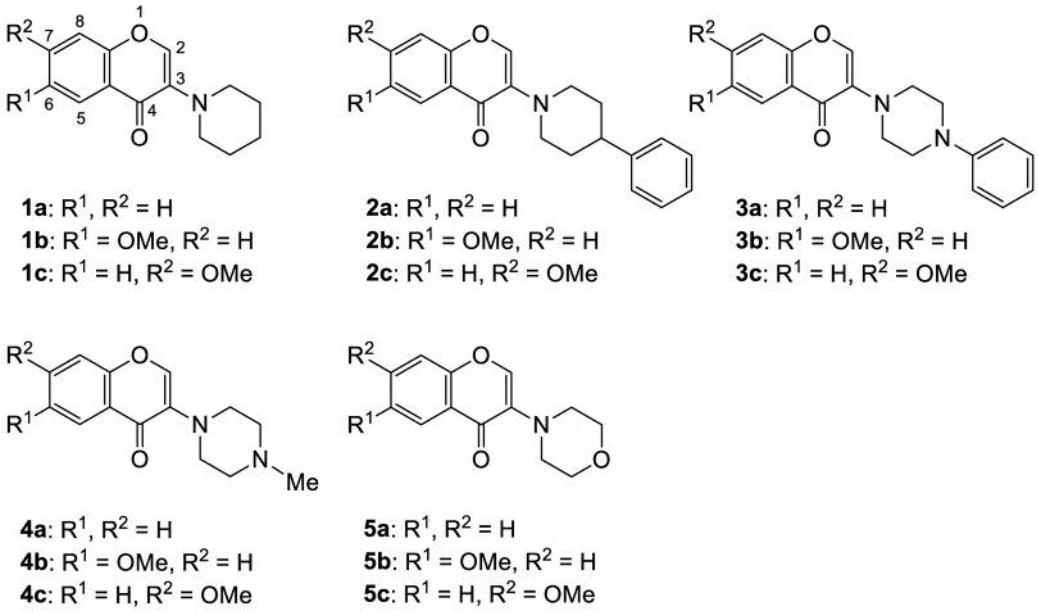

Figure 1. *Structure of 15 3-(N-cyclicamino)chromones investigated in this study.*

tumor specificity, comparable with that of doxorubicin, without induction of apoptosis. Tumor specificity of these derivatives was correlated with molecular shape, especially 3D structure (13).

As far as we know, the biological activity of 3-aminochromones, structural isomers of 2-aminochromones, has not been reported. In continuation of discovering new biological activities of chromone derivatives, we investigated a total of 15 3-(*N*-cyclicamino)chromone derivatives (Figure 1) for their cytotoxicity against four human OSCC cell lines and three human normal oral cell types, and then subjected them to quantitative structure–activity relationship (QSAR) analysis.

Materials and Methods

Materials. The following chemicals and reagents were obtained from the indicated companies: Dulbecco's modified Eagle's medium (DMEM) from GIBCO BRL (Grand Island, NY, USA); fetal bovine serum, 3-(4,5-dimethylthiazol-2-yl)-2,5-diphenyltetrazolium bromide (MTT), doxorubicin, ribonuclease (RNase) A from Sigma-Aldrich Inc. (St. Louis, MO, USA); propidium iodide (PI), dimethyl sulfoxide (DMSO), actinomycin D, and 4% paraformaldehyde phosphate buffer solution from Wako Pure Chem. Ind. (Osaka, Japan); Nonidet-P40 (NP-40) from Nakalai Tesque Inc. (Kyoto, Japan); culture plastic dishes and 96-well plates from Techno Plastic Products AG (Trasadingen, Switzerland).

Synthesis of 3-(N-cyclicamino)chromone derivatives. 3-(1-piperidinyl)-4*H*-1-benzopyran-4-one (**1a**), 6-methoxy-3-(1-piperidinyl)-4*H*-1-benzopyran-4-one (**1b**), 7-methoxy-3-(1-piperidinyl)-4*H*-1-benzopyran-4-one (**1c**), 3-(4-phenyl-1-piperidinyl)-4*H*-1-benzopyran-4-one (**2a**), 6-methoxy-3-(4-phenyl-1-piperidinyl)-4*H*-1-benzopyran-4-one (**2b**), 7-methoxy-3-(4-phenyl-1-piperidinyl)-4*H*-1-benzopyran-4-one (**2c**), 3-(4-phenyl-1-piperazinyl)-4*H*-1-benzopyran-4-one) (**3a**), 6-methoxy-3-(4-phenyl-1-piperazinyl)-4*H*-1-benzopyran-4-one (**3b**), 7-methoxy-3-(4-phenyl-1-piperazinyl)-4*H*-1-benzopyran-4-one (**3c**), 3-(4-methyl-1-piperazinyl)-4*H*-1-benzopyran-4-one (**4a**), 6-methoxy-3-(4-methyl-1-piperazinyl)-4*H*-1-benzopyran-4-one (**4b**), 7-methoxy-3-(4-methyl-1-piperazinyl)-4*H*-1-benzopyran-4-one (**4c**), 3-(4-morpholinyl)-4*H*-1-benzopyran-4-one (**5a**), 6-methoxy-3-(4-morpholinyl)-4*H*-1-benzopyran-4-one (**5b**), 7-methoxy-3-(4-morpholinyl)-4*H*-1-benzopyran-4-one (**5c**) were synthesized by condensation reactions of 2,3-epoxychromone derivatives (14) with selected cyclic secondary amines. All compounds were dissolved in DMSO at 40 mM and stored at –20˚C before use.

Cell culture. Human normal oral mesenchymal cells (human gingival fibroblast, HGF; human periodontal ligament fibroblast, HPLF; and human pulp cells, HPC) were established from the first premolar tooth extracted from the lower jaw of a 12-year-old girl (15), and cells at 10-18 population-doubling levels were used in this study. Human OSCC cell lines [Ca9-22 (derived from gingival tissue); and HSC-2, HSC-3, HSC-4 (derived from tongue)] were purchased from Riken Cell Bank (Tsukuba, Japan). All of these cells were cultured at 37˚C in DMEM supplemented with 10% heat-inactivated fetal bovine serum, 100 units/ml, penicillin G and 100 μg/ml streptomycin sulfate under a humidified 5% CO_2 atmosphere. human oral keratinocytes (purchased from Cosmo Bio Co. Ltd., Tokyo, Japan) were cultured in keratinocyte growth supplement (OKGS, Cat, No. 2652) and cells at 7-11 population-doubling levels were used in the present study. Cell morphology was checked periodically under a light microscope (EVOS FL; Thermo Fisher Scientific, Waltham, MA, USA).

Table I. *Cytotoxic activity of 15 3-(N-cyclicamino)chromones against oral malignant and non-malignant cells. Each value represents the mean of triplicate determinations. Two sets of tumor-specificity index (TS) and potency-selectivity expression (PSE) values were determined using all oral squamous cell carcinoma (OSCC) compared to non-malignant cells, and paired cells derived from the same (gingival) tissue.*

	CC_{50} (μM)														
	Human OSCC cell lines						Human normal oral cells					TS		PSE	
Compound	Ca9-22 (A)	HSC-2	HSC-3	HSC-4	Mean (B)	SD	HGF (C)	HPLF	HPC	Mean (D)	SD	D/B	C/A	$(D/B^2)\times100$	$(C/A^2)\times100$
1a	305	251	268	360	296	48	380	398	>400	393	11	1.3	1.2	0.4	0.4
1b	300	295	278	370	311	41	330	358	323	337	18	1.1	1.1	0.3	0.4
1c	294	281	189	400	291	86	305	308	325	313	11	1.1	1.0	0.4	0.4
2a	43	31	86	40	50	24	358	>400	>400	>386	24	>7.7	8.4	>15.5	19.6
2b	50	22	209	85	92	83	272	181	221	225	45	2.4	5.4	2.7	10.7
2c	93	75	389	400	239	180	>400	>400	>400	>400	0	>1.7	>4.3	>0.7	>4.7
3a	46	20	37	26	32	11	390	>400	>400	>397	6	>12.3	8.5	>38.1	18.4
3b	35	9	176	65	71	74	393	288	317	332	54	4.7	11.3	6.6	32.7
3c	51	9	86	33	45	32	296	350	381	342	43	7.7	5.8	17.3	11.4
4a	>400	>400	350	>400	>388		>400	>400	>400	>400	0	><1.0	><1.0	><0.3	><0.3
4b	>400	>400	>400	>400	>400		>400	>400	>400	>400	0	><1.0	><1.0	><0.3	><0.3
4c	360	324	267	260	303	48	>400	>400	>400	>400	0	>1.3	>1.1	>0.4	>0.3
5a	>400	>400	>400	>400	>400		>400	>400	>400	>400	0	><1.0	><1.0	><0.3	><0.3
5b	>400	>400	>400	>400	>400		>400	>400	>400	>400	0	><1.0	><1.0	><0.3	><0.3
5c	318	>400	389	>400	>377		>400	>400	>400	>400	0	><1.1	>1.3	><0.3	>0.4
Doxorubicin	0.085	0.078	<0.078	<0.078	<0.080		>10	>10	0.50	>6.8		>85.6	>117.2	>107199.7	>137329.1
Melphalan	20	7	7	6	10	6	158	182	153	164	15	16.3	8.0	162.8	40.4

HGF: Human gingival fibroblast; HPLF: human periodontal ligament fibroblast; HPC: human pulp cells; CC_{50}: 50% cytotoxic concentration; DXR: doxorubicin. Ca9-22, derived from gingival tissue; HSC-2, HSC-3 and HSC-4, derived from tongue.

Assay for cytotoxic activity. Cells were inoculated at 2×10^3 cells/0.1 ml in a 96-microwell plate. After 48 h, the medium was replaced with 0.1 ml of fresh medium containing different concentrations of single test compounds. Cells were incubated further for 48 h and the relative viable cell number was then determined by the MTT method (2-5). The relative viable cell number was determined by the absorbance of the cell lysate at 560 nm, using a microplate reader (Infinite F50R; TECAN, Männedorf, Switzerland). Control cells were treated with the same amounts of DMSO and the cell damage induced by DMSO was subtracted from that induced by test agents. The concentration of compound that reduced the viable cell number by 50% (CC_{50}) was determined from the dose–response curve and the mean value of CC_{50} for each cell type was calculated from triplicate assays.

Calculation of tumor-specificity index (TS). TS was calculated using the following equation: TS=mean CC_{50} against three normal oral cell types/mean CC_{50} against OSCC cell lines. Since both Ca9-22 and HGF cells were derived from the gingival tissue (16), the relative sensitivity of these cells was also compared (as: mean CC_{50} against HGF/mean CC_{50} against Ca9-22).

Calculation of potency-selectivity expression (PSE). PSE was calculated by the following equation: PSE=mean CC_{50} against normal oral cell types/(CC_{50} against OSCC cell lines)^2 ×100 (HGF, HPLF *vs*. Ca9-22, HSC-2); and as mean CC_{50} against HGF/(CC_{50} against Ca9-22)^2 ×100 using the pair of cell types from the same tissue (gingiva) (see Table I).

Western blot analysis. Cells were washed with phosphate-buffered saline (PBS) and re-suspended in 50 mM Tris-HCl (pH 7.6), 150 mM NaCl, 1 mM EDTA, 0.1% sodium dodecyl sulfate (SDS), 0.5% deoxycholic acid, 1% NP-40 and protease inhibitors (RIPA buffer). After ultrasonication using Bioruptor (UCD-250; Cosmo Bio) for 12.5 min (10 s on, 20 s off) at 250 W at 4˚C, the soluble cellular extracts were recovered after centrifugation for 10 min at 16,000 × *g*. The protein concentration of each sample was determined using BCA Protein Assay Reagent Kit (Thermo Fisher Scientific) and cell extracts were subjected to western blot analysis. The blots were probed with antibodies to poly (ADP-ribose) polymerase (PARP), caspase 3 (both from Cell Signaling Technology Inc., Beverly, MD, USA) or glyceraldehyde 3-phosphate dehydrogenase (GAPDH) (Trevigen, Gaithersburg, MD, USA), followed by a horseradish peroxidase-conjugated anti-α-rabbit IgG secondary antibody (DAKO, Glostrup, Denmark). The immune complexes were visualized using Pierce Western Blotting Substrate Plus (Thermo Fisher Scientific). Western blot results were documented and quantified using ImageQuant LAS 500 (GE Healthcare, Tokyo, Japan) (17).

Cell-cycle analysis. Treated and untreated cells (approximately 10^6 cells) were harvested, fixed with 1% paraformaldehyde in PBS without calcium and magnesium ions [PBS(−)]. Fixed cells were then washed twice with PBS(−) and treated for 30 min with 400 μl of 0.2 mg/ml RNase A (preheated for 10 min at 100˚C to inactivate DNase) to degrade RNA. Cells were then washed twice with

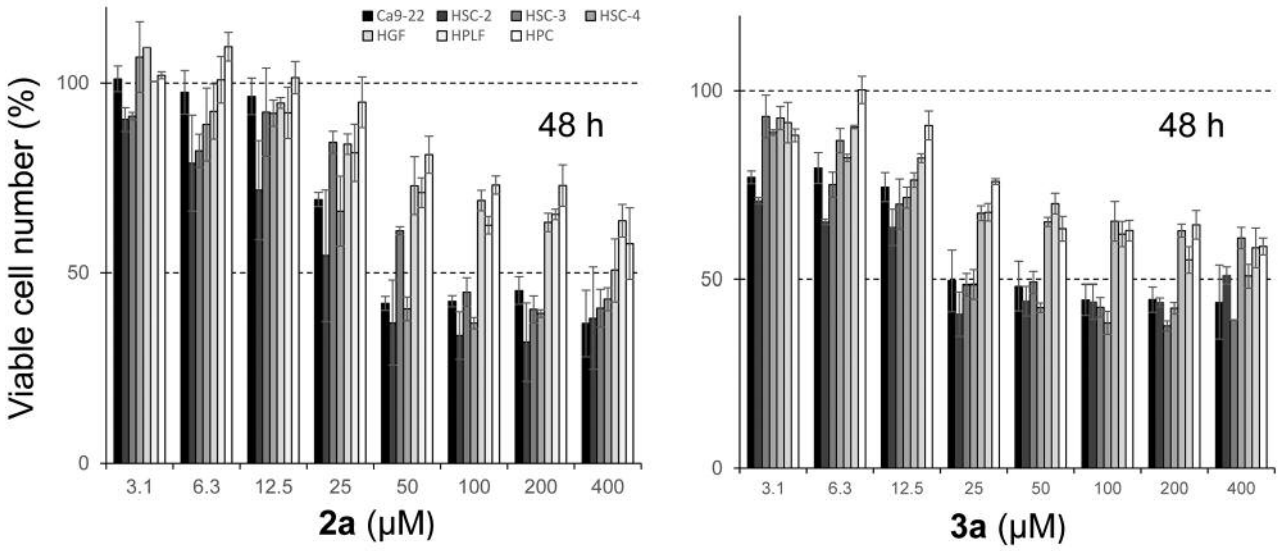

Figure 2. *Cytotoxicity of compounds **2a** and **3a** against four human oral squamous cell carcinoma cell lines Ca9-22, HSC-2, HSC-3 and HSC-4, and human normal oral cells human gingival fibroblast (HGF), human periodontal ligament fibroblast (HPLF) and human pulp cells (HPC). Cells were incubated for 48 h without (control) or with the indicated concentrations of **2a** (left) or **3a** (right), and cell viability was determined by the MTT method, and expressed as a percentage that of the control. Each value represents the mean±S.D. of triplicate assays.*

Table II. *Toxicity of compound **3a** against human oral keratinocytes (HOK) and human oral squamous cell carcinoma (OSCC) cell lines compared to doxorubicin.*

	CC_{50} (mM)		
	OSCC	HOK	TS
2-(4-Phenyl-1-piperazinyl)-4*H*-1-benzopyran-4-one (**3a**) (This study)	32.3	400	12.4
7-Methoxy-2-(4-morpholinyl)-4*H*-1-benzopyran-4-one (**5c**) [cf (13)]	5.5	357.7	65.2
Doxorubicin	0.08	0.119	1.5

CC_{50}: 50% Cytotoxic concentration; TS: tumor-specificity.

PBS(−) and stained for 15 min with 0.01% propidium iodide (PI) in the presence of 0.01% NP-40 in PBS(−) – to prevent cell aggregation. After filtering through Falcon® cell strainers (40 μM) (Corning, NY, USA) to remove aggregated cells, PI-stained cells were subjected to cell sorting (SH800 Series; SONY Imaging Products and Solutions Inc., Kanagawa, Japan). Cell-cycle analysis was performed with Cell Sorter Software version 2.1.2. (SONY Imaging Products and Solution Inc.).

Estimation of CC_{50} values. Since the CC_{50} values had a distribution pattern close to a logarithmically normal distribution, we used the negative log CC_{50} (pCC_{50}) values for the comparison of cytotoxicity between compounds. The mean pCC_{50} values for normal cells and tumor cell lines were defined as N and T, respectively (3).

Calculation of chemical descriptors. The 3D structure of each chemical structure (Marvin Sketch ver 16; ChemAxon, Budapest, Hungary, http://www.chemaxon.com) was optimized by CORINA Classic (Molecular Networks GmbH, Nürnberg, Germany) with forcefield calculations (amber-10: EHT) in Molecular Operating Environment (MOE) version 2018.0101 (Chemical Computing Group Inc., Quebec, Canada). The number of structural descriptors calculated

Table III. *Number of descriptors showing significant correlation with mean negative log of the concentration of compound that reduced the viable cell number by 50% (pCC_{50}) for tumor cells (T), normal cells (N) and normal cells versus tumor cells (T−N).*

	Level of significance	
Property	$p<0.05$	$p<0.005$
T	2,296	1,890
N	144	9
T−N	2,206	1,713

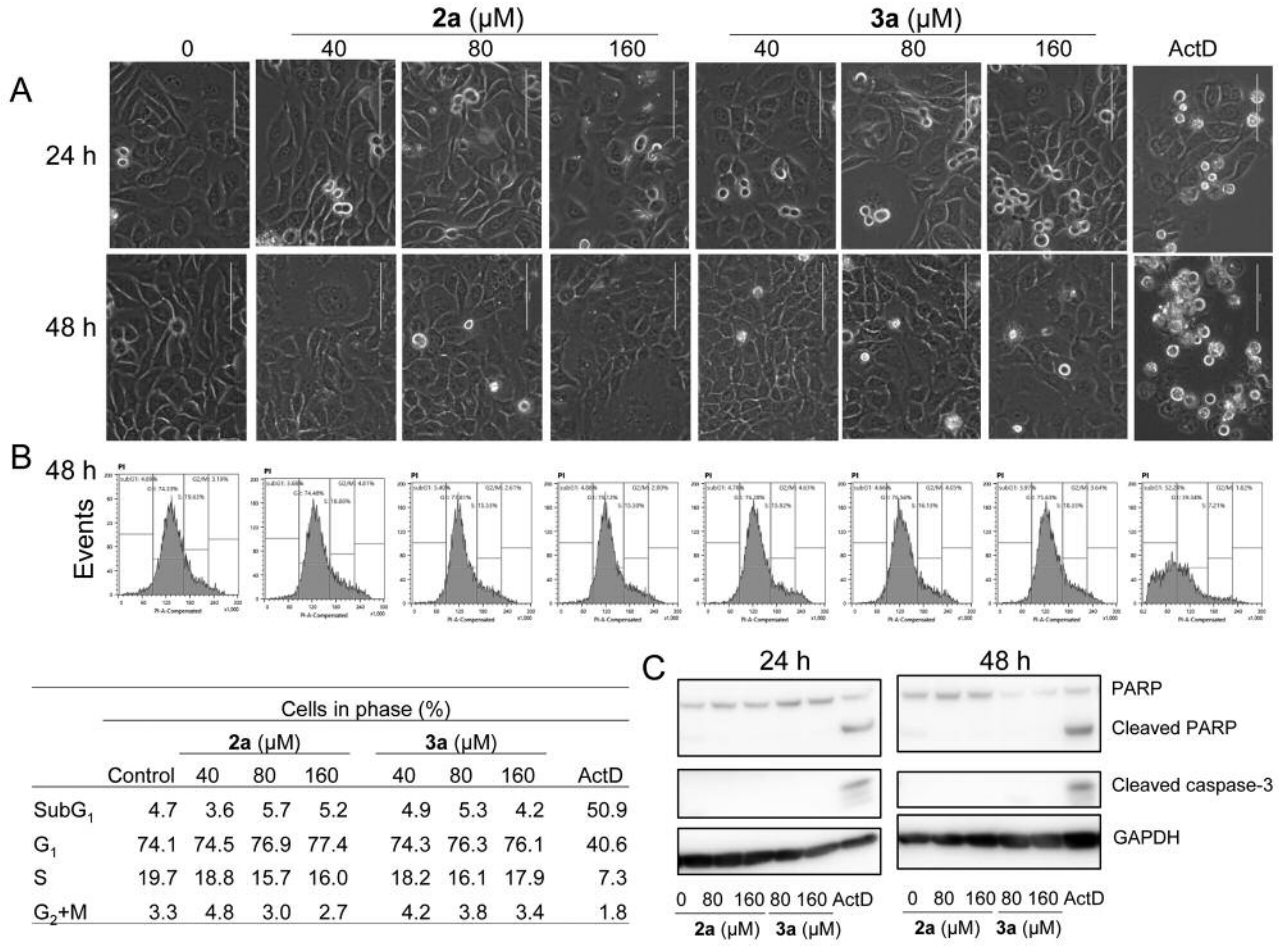

	Cells in phase (%)							
		2a (μM)			3a (μM)			
	Control	40	80	160	40	80	160	ActD
$SubG_1$	4.7	3.6	5.7	5.2	4.9	5.3	4.2	50.9
G_1	74.1	74.5	76.9	77.4	74.3	76.3	76.1	40.6
S	19.7	18.8	15.7	16.0	18.2	16.1	17.9	7.3
G_2+M	3.3	4.8	3.0	2.7	4.2	3.8	3.4	1.8

Figure 3. *Effect of **3a** on cell morphology (A), apoptosis induction (B) and cell-cycle analysis (C) in oral squamous cell carcinoma cell line HSC-2. Cells were incubated for 24 or 48 h with the indicated concentrations of **3a** or 1 μM actinomycin D (Act D) as positive control and then assessed for morphology under light microscopy (EVOS FL; Thermo Fisher Scientific), cell-cycle distribution by cell sorting and apoptosis induction by western blot. Bar=100 μm. GAPDH: Glyceraldehyde 3-phosphate dehydrogenase; PARP: poly (ADP-ribose) polymerase.*

from MOE (18) and Dragon 7.0 (19) (Kode srl., Pisa, Italy) was 344 and 5,255, respectively. Among them, the number of descriptors used for analysis was 302 and 2,794 (total 3,096), respectively.

Statistical treatment. The CC_{50} values were expressed as mean±S.D. of triplicate assays. The relation among cytotoxicity, TS and chemical descriptors was investigated using simple regression analyses by JMP Pro version 13.2.0 (SAS Institute Inc., Cary, NC, USA). The significance level was set at $p<0.05$.

Results

Cytotoxicity. A total of 15 3-(*N*-cyclicamino)chromone derivatives were synthesized, without (A series) or with the introduction of methoxy group at the C-6 position (B series) or the C-7 position (C series) of the benzopyran-4-one (chromone) ring attached by 1-piperidinyl (**1a, 1b, 1c**), 4-phenyl-1-piperidinyl (**2a, 2b, 2c**), 4-phenyl-1-piperazinyl (**3a, 3b, 3c**), 4-methyl-1-piperazinyl (**4a, 4b, 4c**) or 4-morpholinyl (**5a, 5b, 5c**) group at the C-3 position (Figure 1).

We first investigated the effect of introduction of substituent groups at the C-3 position on the induction of cytotoxicity of chromone. The compound with a 4-phenyl-1-piperazinyl group (**3a**) had the highest cytotoxicity against four human OSCC cell lines (mean CC_{50}=32 μM), followed by compounds with 4-phenyl-1-piperidinyl (**2a**), 1-piperidinyl (**1a**), and then those with 4-methyl-1-piperazinyl group (**4a**) and 4-morpholinyl (**5a**) (>400 μM). These compounds showed very weak cytotoxicity against human normal oral cells (HGF, HPLF, HPC) (CC_{50} >386 μM) (Table I).

Introduction of a methoxy group at the C-6 position of **2a** and **3a** did not further increase, but rather reduced their cytotoxicity against OSCC cells (compare with **2b** and **3b**, Table I). Introduction of a methoxy group to the C-7 position

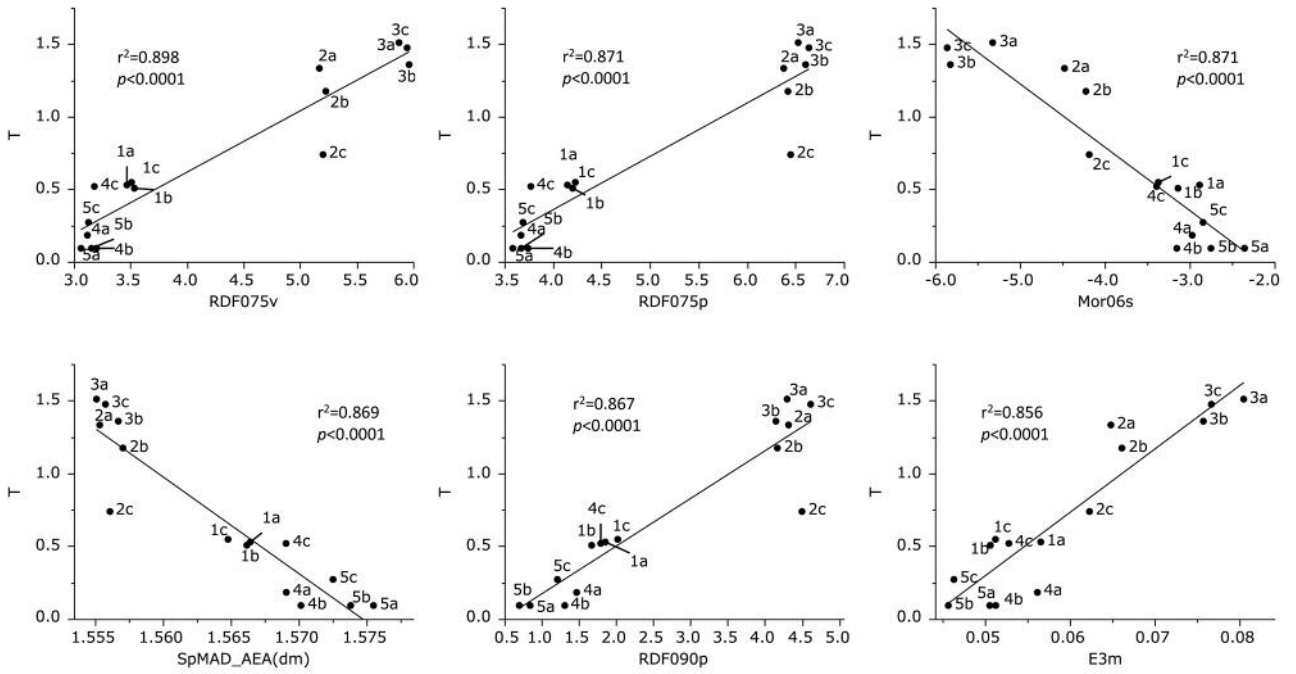

Figure 4. *Determination of correlation coefficient between chemical descriptors and cytotoxicity of 15 3-(N-cyclicamino)chromones against tumor cells. The mean negative log of the concentration of compound that reduced the viable cell number by 50% (CC_{50}) values (T) against tumor cells were plotted. The following chemical descriptors were used: RDF075v, E3m: shape and size; RDF075p, RDF090p: shape and polarizability; Mor06s: 3D shape and electric state; SpMAD_AEA(dm): shape and dipole moment.*

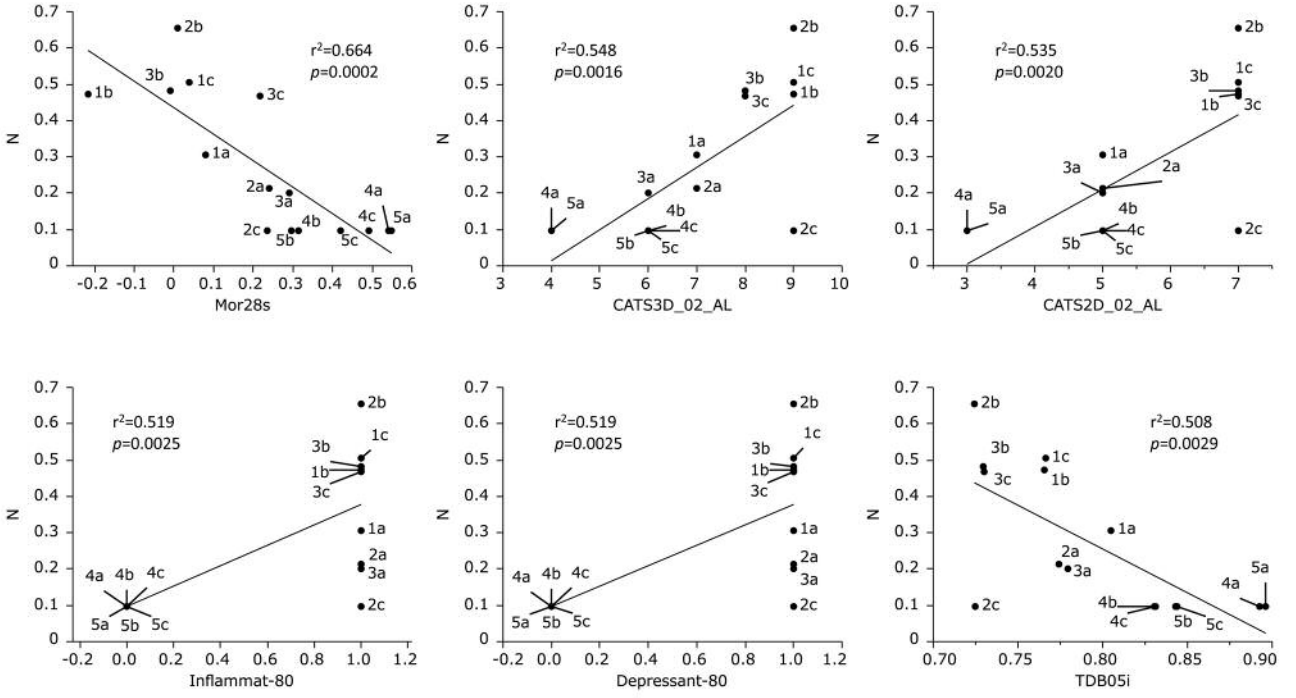

Figure 5. *Determination of correlation coefficient between chemical descriptors and cytotoxicity of 15 3-(N-cyclicamino)chromones against normal cells. The mean negative log of the concentration of compound that reduced the viable cell number by 50% (CC_{50}) values (N) against normal cells were plotted. The following chemical descriptors were used: Mor28s: 3D shape and electric state; CATS2D_02_AL, CATS3D_02_AL: hydrogen-bond acceptor and lipophilicity, Inflammat-80, Depressant-80: drug-likeness; TDB05i: 3D shape and ionization potential.*

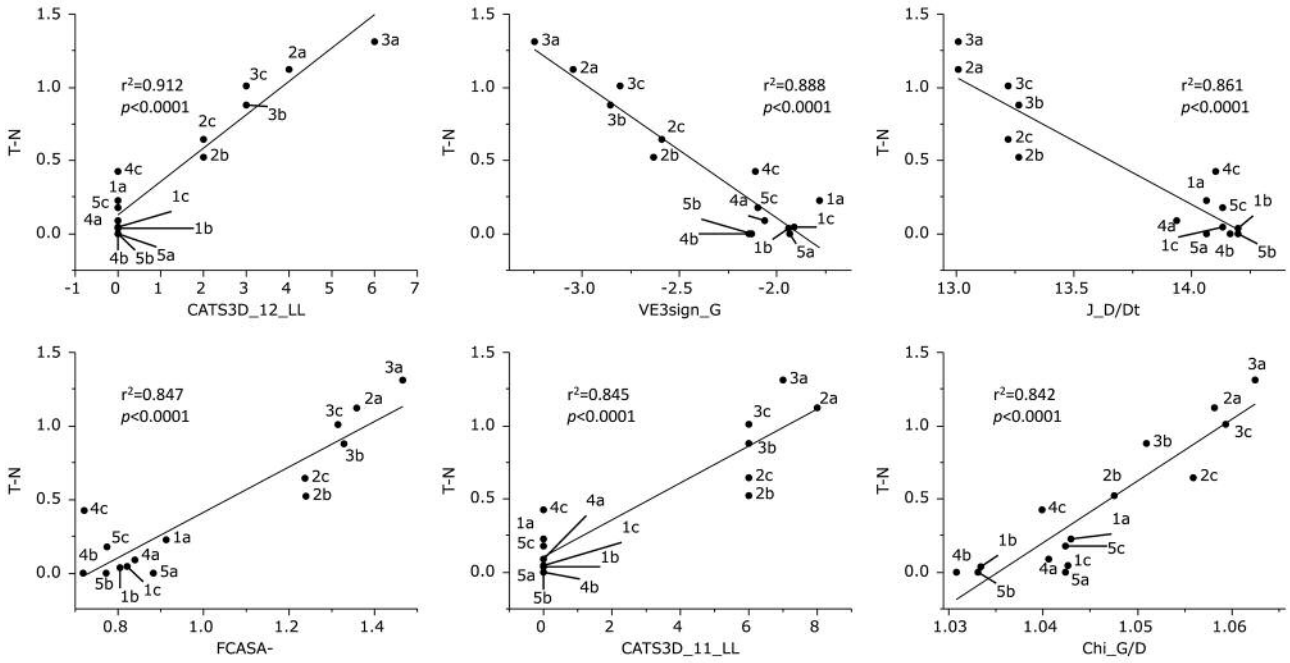

Figure 6. *Determination of correlation coefficient between chemical descriptors and tumor specificity of 15 3-(N-cyclicamino)chromones [defined as: cytotoxicity against tumor cells−cytotoxicity against normal cells (T−N)]. The following chemical descriptors were used: CATS3D_11_LL, CATS3D_12_LL: lipophilicity; VE3sign_G, Chi_G/D: 3D shape; J_D/Dt: shape; FCASA-: shape and negative charge.*

of **2a** and **3a** also failed to increase cytotoxicity against OSCC cells (compare with **2c** and **3c**, Table I).

Tumor specificity. Among 15 compounds, **3a** had the highest TS (TS>12.3), followed by **2a** (TS>7.7) and then **3b** (TS=4.7). The TS values of other compounds was below 3 (Table I). The TS value of **3a** was much lower than that for doxorubicin (TS>85.6), but very close to that of melphalan (TS=16.3). Compound **3a** caused cytostatic growth inhibition of OSCC cells (Figure 2). Furthermore, **3a** was much less cytotoxic against human oral keratinocytes as compared with doxorubicin (Table II).

Considering that HGF is the normal cell type corresponding to Ca9-22 OSCC cell line (since both derive from gingival tissues), TS values were also generated by dividing the average CC_{50} value towards HGF cells by the CC_{50} value towards Ca9-22 cells (C/A, Table I). The TS values derived in this way for **3a** (TS=8.5) and **2a** (TS=8.4) were slightly higher than that of melphalan (TS=8.0) (Table I).

PSE value. In order to identify the most promising compounds in terms of both good potency and selectively cytotoxicity, PSE values were calculated. PSE values of **2a** and **3a** (>15.5 and >38.1) against malignant cells were 9.5% and 23.4% that of melphalan (PSE=162.8), respectively. For gingival tissue, PSE values of **2a** and **3a** (PSE=19.6 and 18.4) were 48.5% and 45.5% that of melphalan (PSE=40.4), respectively (Table I).

*Type of cell death induced by **3a***. When HSC-2 cells were incubated for 24 h with increasing concentrations (20, 40, 80 or 160 μM) of **3a**, cells became gradually enlarged (upper column in Figure 3A). In contrast, actinomycin D treatment induced cell shrinkage, characteristic of apoptosis (Figure 3A).

Cell-cycle analysis demonstrated that actinomycin D, but not **2a** nor **3a**, produced significantly ($p<0.001$) higher proportions of sub-G_1 cells (50.9±1.3%) *vs*. control (4.0±0.01%), a characteristic feature of apoptotic cells (Figure 3B). These data indicate apoptosis induction by **2a** and **3a** is unlikely.

Western blot analysis demonstrated that **3a** did not lead to caspase-3 activation, as evidenced by lack of cleavage PARP and caspase-3, in contrast to actinomycin D treatment (Figure 3C).

Computational analysis. We next performed the QSAR analysis of the 15 3-(*N*-cyclicamino)chromones in regards to their cytotoxicity against tumor cells and normal cells. Since so many chemical descriptors were significantly correlated with cytotoxicity and TS ($p<0.05$ and $p<0.005$, respectively) (Table III), the top six chemical descriptors were chosen for QSAR analysis (Figures 4-6, and Table IV).

The cytotoxicity of 15 3-(*N*-cyclicamino)chromones against human OSCC cell lines was correlated positively with RDF075v

Table IV. *Properties of descriptors that significantly affected cytotoxicity against tumor cells (T) and normal cells (N), and tumor specificity (T−N).*

	Descriptor	Source	Meaning	Explanation
T	RDF075v	Dragon	Shape and size	Radial distribution function-075/weighted by van der Waal's volume RDF
	RDF075p	Dragon	Shape and polarizability	Radial distribution function-075/weighted by polarizability
	Mor06s	Dragon	3D shape and electric state	Signal 06/weighted by I-state
	SpMAD_AEA(dm)	Dragon	Shape and dipole moment	Spectral mean absolute deviation from augmented edge adjacency mat. weighted by dipole moment
	RDF090p	Dragon	Shape and polarizability	Radial distribution function-090/weighted by polarizability
	E3m	Dragon	Shape and size	3rd component accessibility directional WHIM index/weighted by mass
N	Mor28s	Dragon	3D Shape and electric state	Signal 28/weighted by I-state
	CATS3D_02_AL	Dragon	Hydrogen-bond acceptor and lipophilicity	CATS3D Acceptor-lipophilic BIN 02 (2.000-3.000Å)
	CATS2D_02_AL	Dragon	Hydrogen-bond acceptor and lipophilicity	CATS2D Acceptor-lipophilic at lag 02
	Inflammat-80	Dragon	Drug-likeness	Ghose-Viswanadhan-Wendoloski anti-inflammatory-like index at 80%
	Depressant-80	Dragon	Drug-likeness	Ghose-Viswanadhan-Wendoloski antidepressant-like index at 80%
	TDB05i	Dragon	3D shape and ionization potential	3D Topological distance based descriptors-lag 5 weighted by ionization potential
T-N	CATS3D_12_LL	Dragon	Lipophilicity	CATS3D Lipophilic-Lipophilic BIN 12 (12.000-13.000Å)
	VE3sign_G	Dragon	3D shape	Logarithmic coefficient sum of the last eigenvector from geometrical matrix
	J_D/Dt	Dragon	Shape	Balaban-like index from distance/detour matrix
	FCASA-	MOE	Shape and negative charge	Fractional CASA-(negative charge weighted surface area, ASA-times max {qi<0}) calculated as CASA-/accessible surface area.
	CATS3D_11_LL	Dragon	Lipophilicity	CATS3D lipophilic-lipophilic BIN 11 (11.000-12.000Å)
	Chi_G/D	Dragon	3D shape	Randic-like index from distance/distance matrix

(shape and size) (r^2=0.898, p<0.0001), RDF075p (shape and polarizability) (r^2=0.871, p<0.0001), RDF090p (shape and polarizability) (r^2=0.867, p<0.0001) and E3m (shape and size) (r^2=0.856, p<0.0001), while negatively with Mor06s (3D shape and electric state) (r^2=0.871, p<0.0001) and SpMAD_AEA(dm) (shape and dipole moment) (r^2=0.869, p<0.0001) (Figure 4).

The cytotoxicity of 15 3-(*N*-cyclicamino)chromones against human normal oral mesenchymal cells was correlated positively with CATS3D_02_AL (hydrogen-bond acceptor and lipophilicity) (r^2=0.548, p=0.0016), CATS2D_02_AL (hydrogen-bond acceptor and lipophilicity) (r^2=0.535, p=0.0020), Inflammat-80 (drug-likeness) (r^2=0.519, p=0.0025) and Depressant-80 (drug-likeness) (r^2=0.519, p=0.0025), while negatively with Mor28s (3D shape and electoric state) (r^2=0.664, p=0.0002) and TDB05i (3D shape and ionization potential) (r^2=0.508, p=0.0029) (Figure 5).

The TS of 15 3-(*N*-cyclicamino)chromones was correlated positively with CATS3D_12_LL (lipophilicity) (r^2=0.912, p<0.0001), FCASA-(shape and negative charge) (r^2=0.847, p<0.0001), CATS3D_11_LL (lipophilicity) (r^2=0.845, p<0.0001) and Chi_G/D (3D shape) (r^2=0.842, p<0.0001), while negatively with VE3sign_G (3D shape) (r^2=0.888, p<0.0001) and J_D/Dt (shape) (r^2=0.861, p<0.0001) (Figure 6).

Discussion

The present study demonstrated for the first time that among 15 3-(*N*-cyclicamino)chromones, (**2a** and **3a** had the highest tumor specificity, comparable with that of melphalan (Table I). Furthermore, **3a** was much less cytotoxic against human normal oral keratinocytes compared with doxorubicin. We found that these compounds led to cytostatic growth inhibition, only reducing the viable cell number by 60% after 48 h (Figure 2). Compound **3a** did not produce an increased G_1 cell population nor induced caspase-3 activation, suggesting that **3a** does not induce apoptotic cell death.

We recently reported that 7-methoxy-2-(4-morpholinyl)-4*H*-1-benzopyran-4-one [**5c** which had the highest tumor specificity among 15 2-(*N*-cyclicamino)chromone derivatives (13)], led to cytotoxic growth inhibition in OSCC cell lines without induction of apoptosis. These results suggest that these structural isomers, 2-(*N*-cyclicamino)chromones and 3-(*N*-cyclicamino)chromones, have no apoptosis-inducing activity, despite exhibiting different modes of growth inhibition (either cytotoxic or cytostatic). There are a variety of types of cell death reported (20). Further study is needed to determine which type of cell death **3a** induces in human OSCC cell lines.

QSAR analysis demonstrated that cytotoxicity of 15 3-(*N*-cyclicamino)chromones against tumor cell lines was highly significantly correlated with descriptors of shape, size, polarizability, electric state, and dipole moment (p-values from 8.03×10^{-7} to 8.42×10^{-8}) (Figure 4). Their tumor specificity was also significantly positively correlated lipophilicity, 3D shape, and negative charge (p-values from 1.45×10^{-6} to 3.18×10^{-8}) (Figure 6). Taken together, these data suggest that

tumor specificity is positively related with chemical descriptors that reflect 3D structure and lipophilicity.

When we compared the A series of compounds of 3-(*N*-cyclicamino)chromones (this study) with their structural isomers, 2-(*N*-cyclicamino)chromones (13), there were common properties: 4-phenyl-1-piperazinyl derivatives (**3a**) of both groups had the highest cytotoxicity against four human OSCC cell lines, followed by 4-phenyl-1-piperidinyl derivatives (**2a**) in both cases [Table I and (13)]. Furthermore, TS of both groups of compounds were correlated with 3D structure (mass or shape) reflected by Mor17v, Mor17m and Mor22m for 2-(*N*-cyclicamino)chromones, and FCASA-, Chi_G/D, VE3sign_G, J_D/Dt for 3-(*N*-cyclicamino) chromones. In addition, we found that both **3a** (this study) and 7-methoxy-2-(4-morpholinyl)-4*H*-1-benzopyran-4-one [**5c**, described as the most tumor-specific compound among 15 2-(*N*-cyclicamino)chromones (13)] were much less toxic towards human oral keratinocytes compared with doxorubicin (Table II), further substantiating them as new promising anticancer drug candidates.

Chemical modification using **3a** as a lead compound may be a potential choice for designing a new type of anticancer drug.

Conflicts of Interest

The Authors wish to confirm that there are no known conflicts of interest associated with this publication and there has been no significant financial support for this work that could have influenced its outcome.

Acknowledgements

This work was partially supported by KAKENHI from the Japan Society for the Promotion of Science (JSPS) (15K08111, 16K11519).

References

1 Gaspar A, Matos MJ, Garrido J, Uriarte E and Borges F: Chromone: A valid scaffold in medicinal chemistry. Chem Rev *114(9)*: 4960-4992, 2014.

2 Shimada C, Uesawa Y, Ishii-Nozawa R, Ishihara M, Kagaya H, Kanamto T, Terakubo S, Nakashima H, Takao K, Sugita Y and Sakagami H: Quantitative structure–cytotoxicity relationship of 3-styrylchromones. Anticancer Res *34*: 5405-5412, 2014.

3 Uesawa Y, Sakagami H, Ishihara M, Kagaya H, Kanamoto T, Terakubo S, Nakashima H, Yahagi H, Takao K and Sugita Y: Quantitative structure–cytotoxicity relationship of 3-styryl-2*H*-chromenes. Anticancer Res *35*: 5299-5308, 2015.

4 Sakagami H, Okudaira N, Uesawa Y, Takao K, Kagaya H and Sugita Y: Quantitative structure-cytotoxicity relationship of 2-azolylchromones. Anticancer Res *38(2)*: 763-770, 2018.

5 Sakagami H, Okudaira N, Masuda Y, Amano O, Yokose S, Kanda Y, Suguro M, Natori T, Oizumi H and Oizumi T: Induction of apoptosis in human oral keratinocyte by doxorubicin. Anticancer Res *37(3)*: 1023-1029, 2017.

6 Mazzei M, Sottofattori E, Dondero R, Ibrahim M, Melloni E and Michetti M: *N,N*-Dialkylaminosubstituted chromones and isoxazoles as potential anti-inflammatory agents. Il. Farmaco *54*: 452-460, 1999.

7 Hatnapure GD, Keche AP, Rodge AH, Birajdar SS, Tale RH and Kamble VM: Synthesis and biological evaluation of novel piperazine derivatives of flavone as potent anti-inflammatory and antimicrobial agent. Bioorg Med Chem Lett *22(20)*: 6385-6390, 2012.

8 Abbott BM and Thompson PE: PDE2 inhibition by the PI3 kinase inhibitor LY294002 and analogues. Bioorg Med Chem Lett 14: 2847-2851, 2004.

9 Roma G, Di Braccio M, Grossi G, Piras D, Leoncini G, Bruzzese D, Signorello MG, Fossa P and Mosti L: Synthesis and *in vitro* antiplatelet activity of new 4-(1-piperazinyl)coumarin derivatives. Human platelet phosphodiesterase 3 inhibitory properties of the two most effective compounds described and molecular modeling study on their interactions with phosphodiesterase 3A catalytic site. J Med Chem *50(12)*: 2886-2895, 2007.

10 Raymond M, FinlayaRoger V and Griffinb J: Modulation of DNA repair by pharmacological inhibitors of the PIKK protein kinase family. Bioorg Med Chem Lett *22(17)*: 5352-5359, 2012.

11 Griffin RJ, Fontana G, Golding BT, Guiard S, Hardcastle IR, Leahy JJ, Martin N, Richardson C, Rigoreau L, Stockley M and Smith GC: Selective benzopyranone and pyrimido[2,1-a]isoquinolin-4-one inhibitors of DNA-dependent protein kinase: synthesis, structure-activity studies, and radiosensitization of a human tumor cell line *in vitro*. J Med Chem *48(2)*: 569-585, 2005.

12 Gao M, Wang M, Miller KD and Zheng QH: Simple synthesis of carbon-11-labeled chromen-4-one derivatives as new potential PET agents for imaging of DNA-dependent protein kinase (DNA-PK) in cancer. Appl Radiat Isot *70(8)*: 1558-1563, 2012.

13 Shi H, Nagai J, Sakatsume T, Bandow K, Okudaira N, Sakagami H, Tomomura M, Tomomura A, Uesawa Y, Takao K and Sugita Y: Quantitative structure–cytotoxicity relationship of 2-(*N*-cyclicamino)chromone derivatives. Anticancer Res *38(7)*: 3897-3906, 2018.

14 Spadafora M, Postupalenko VY, Shvadchak VV, Klymchenko AS, Mély Y, Burger A and Benhida R: Efficient synthesis of ratiometric fluorescent nucleosides featuring 3-hydroxychromone nucleobases. Tetrahedron *65*: 7809-7816, 2009.

15 Kantoh K, Ono M, Nakamura Y, Nakamura Y, Hashimoto K, Sakagami H and Wakabayashi H: Hormetic and anti-radiation effects of tropolone-related compounds. In Vivo *24*: 843-852, 2010.

16 Horikoshi M, Kimura Y, Nagura H, Ono T and Ito H: A new human cell line derived from human carcinoma of the gingiva. I. Its establishment and morphological studies. Jpn J Oral Maxillofac Surg *20*: 100-106, 1974.

17 Tomikoshi Y, Nomura M, Okudaira N, Sakagami H and Wakabayashi H: Enhancement of cytotoxicity of three apoptosis-inducing agents against human oral squamous cell carcinoma cell line by benzoxazinotropone. In Vivo *30(5)*: 645-650, 2016.

18 Calculate Descriptors, MOE2015.10 on-line help manual, Chemical Computing Group.

19 https://chm.kode-solutions.net/products_dragon_descriptors.php

20 Fricker M, Tolkovsky AM, Borutaite V, Coleman M and Brown GC: Neuronal cell death. Physiol Rev *98(2)*: 813-880, 2018.

Received June 8, 2018
Revised July 1, 2018
Accepted July 4, 2018